AMERICAN SOCIETY FOR MICROBIOLOGY | Infection and Immunity

Effects of B Cell Depletion on Early *Mycobacterium tuberculosis* Infection in Cynomolgus Macaques

Jiayao Phuah,[a]* Eileen A. Wong,[a] Hannah P. Gideon,[a] Pauline Maiello,[a] M. Teresa Coleman,[a] Matthew R. Hendricks,[a] Rachel Ruden,[b] Lauren R. Cirrincione,[c] John Chan,[d] Philana Ling Lin,[e] JoAnne L. Flynn[a]

Department of Microbiology and Molecular Genetics, University of Pittsburgh School of Medicine, Pittsburgh, Pennsylvania, USA[a]; University of Pennsylvania School of Veterinary Medicine, Philadelphia, Pennsylvania, USA[b]; University of Pittsburgh School of Pharmacy, Pittsburgh, Pennsylvania, USA[c]; Department of Medicine and Microbiology and Immunology, Albert Einstein College of Medicine, Bronx, New York, USA[d]; Department of Pediatrics, Children's Hospital of Pittsburgh of the University of Pittsburgh Medical Center, Pittsburgh, Pennsylvania, USA[e]

Although recent studies in mice have shown that components of B cell and humoral immunity can modulate the immune responses against *Mycobacterium tuberculosis*, the roles of these components in human and nonhuman primate infections are unknown. The cynomolgus macaque (*Macaca fascicularis*) model of *M. tuberculosis* infection closely mirrors the infection outcomes and pathology in human tuberculosis (TB). The present study used rituximab, an anti-CD20 antibody, to deplete B cells in *M. tuberculosis*-infected macaques to examine the contribution of B cells and humoral immunity to the control of TB in nonhuman primates during the acute phase of infection. While there was no difference in the overall pathology, disease profession, and clinical outcome between the rituximab-treated and untreated macaques in acute infection, analyzing individual granulomas revealed that B cell depletion resulted in altered local T cell and cytokine responses, increased bacterial burden, and lower levels of inflammation. There were elevated frequencies of T cells producing interleukin-2 (IL-2), IL-10, and IL-17 and decreased IL-6 and IL-10 levels within granulomas from B cell-depleted animals. The effects of B cell depletion varied among granulomas in an individual animal, as well as among animals, underscoring the previously reported heterogeneity of local immunologic characteristics of tuberculous granulomas in nonhuman primates. Taken together, our data clearly showed that B cells can modulate the local granulomatous response in *M. tuberculosis*-infected macaques during acute infection. The impact of these alterations on disease progression and outcome in the chronic phase remains to be determined.

Studies of protective immunity against *Mycobacterium tuberculosis* have focused mainly on T cells. The relative contribution of B cells and antibody in control of *M. tuberculosis* infection in humans or nonhuman primates remain relatively unknown. Emerging evidence suggests that B cell and humoral immunity play important roles in shaping immune responses to *M. tuberculosis* (1). B cells are a conspicuous cellular component of the lung granulomatous response in tuberculous mice (2–7), nonhuman primates (2, 8), and humans (2, 3, 9, 10). B cells form prominent aggregates with characteristic features of the germinal center (2, 4, 7, 9, 10). B cell-deficient mice display enhanced susceptibility to *M. tuberculosis*, as assessed by tissue bacterial burden (4, 11), which is associated with aberrant lung cytokine (4) and granulomatous inflammatory response (4, 12, 13), as well as tissue neutrophilia (4, 13). Of note, there is evidence suggesting that the inflammation regulatory role of B cells during *M. tuberculosis* infection can be strain and infection phase specific (4, 12, 13). Studies using specific Fcγ receptor knockout mouse strains have shown that signaling through distinct receptors can differentially regulate susceptibility to *M. tuberculosis*, as measured by tissue bacterial load, and lung cytokine production, suggesting a role for immunoglobulins in regulating the immune response to the pathogen (14). Indeed, enhanced susceptibility to *M. tuberculosis* that is associated with aberrant lung cytokine production has been observed in agammaglobulinemic AID$^{-/-}$ μS$^{-/-}$ mice (15). Treatment with a number of monoclonal antibodies against specific mycobacterial components has been shown to be protective against challenge with *M. tuberculosis* (16), and coating *M. tuberculosis* bacilli with a monoclonal antibody of the IgG3 isotype against arabinomannan attenuated virulence relative to uncoated bacilli (17).

The present study explored the effects of B cell depletion in the cynomolgus macaque model of tuberculosis (TB) (18, 19). Cynomolgus macaques recapitulate the full infection outcome and pathological spectrum of *M. tuberculosis* infection seen in humans. Like humans, macaques are extremely variable in their response to *M. tuberculosis* infection, with substantial animal-to-animal and within-animal variability in terms of immune responses and bacterial numbers. We published previously that CFU per granuloma varied from 0 to 10^5 within individual animals, and T cell responses were equally variable in granulomas from an individual animal. This variability suggests that local mechanisms of control of infection, and the immune responses necessary for control of *M. tuberculosis* differ from granuloma to

Received 2 February 2016 **Accepted** 6 February 2016

Accepted manuscript posted online 16 February 2016

Citation Phuah J, Wong EA, Gideon HP, Maiello P, Coleman MT, Hendricks MR, Ruden R, Cirrincione LR, Chan J, Lin PL, Flynn JL. 2016. Effects of B cell depletion on early *Mycobacterium tuberculosis* infection in cynomolgus macaques. Infect Immun 84:1301–1311. doi:10.1128/IAI.00083-16.

Editor: S. Ehrt

Address correspondence to JoAnne L. Flynn, joanne@pitt.edu.

* Present address: Jiayao Phuah, Department of Microbiology and Physiological Systems, University of Massachusetts Medical School, Worcester, Massachusetts, USA.

Supplemental material for this article may be found at http://dx.doi.org/10.1128/IAI.00083-16.

granuloma, even within the same animal. We suspect similar or even higher levels of variability in humans. Thus, in this model there are several features that can be assessed: overall pathology and bacterial burden, individual granuloma and lymph node bacterial burden and immune responses, and inflammation via positron emission tomography-computed tomography (PET/CT) imaging.

B cell depletion can be achieved by the administration of anti-human CD20 chimeric monoclonal antibody, rituximab (20). Rituximab is in clinical use for the treatment of certain B cell lymphomas and autoimmune conditions such as systemic lupus erythematosis, rheumatoid arthritis, and multiple sclerosis (21). B cells are thought to be depleted via antibody-dependent cell-mediated cytotoxicity mode of clearance by natural killer cells (22). Although rituximab use can predispose patients toward certain infections, the available clinical data do not indicate an increased risk of TB associated with rituximab (23). However, rituximab is used most extensively in countries where tuberculosis is not endemic, safety studies excluded *M. tuberculosis*-infected persons, and in studies with TB patients anti-TB drugs were used with rituximab, which would dramatically reduce the risk of disease.

Rituximab has been used in nonhuman primate research, particularly in animal models of simian immunodeficiency virus (SIV) infection, and is known to be effective at depleting nonhuman primate B cells (20, 24, 25). Although B cells are depleted, rituximab has not been observed to interfere with the plasma cell compartment, since these cells are not generally $CD20^+$. Hence, preexisting antibody responses would not be affected by rituximab, although further antigen-specific antibody generation would be impaired. This study was undertaken to help elucidate the contribution of B cells and antigen-specific antibodies to the control of TB in a model similar to humans. The results revealed that while rituximab treatment did not alter the overall disease progression and outcome of *M. tuberculosis*-infected macaques during the acute phase of the infection, the study showed that the B cell compartment can significantly modulate various aspects of immune responses to *M. tuberculosis* in acute infection, impacting bacterial load cytokine profiles and inflammation levels. Such findings form the basis from which additional insights into the role of B cells and humoral immunity regulate the immune response to *M. tuberculosis*, which can potentially guide the development of efficacious vaccines or novel treatment modalities.

MATERIALS AND METHODS

Experimental animals and B-cell depletion. A total of 16 adult (>4 years of age) cynomolgus macaques (*Macaca fascicularis*; Covance, Alice, TX; USA Valley Biosystems, West Sacramento, CA) were obtained for the B cell studies described here. The 16 animals were divided into eight pairs in which one animal receives rituximab and the other receives saline as a control and the animals are infected at the same time.

Rituximab (Genentech, San Francisco, CA) was administered at a dosage of 50 mg/kg over a period of 45 min with the first dose given 2 weeks prior to *M. tuberculosis* infection. Subsequent doses of rituximab were administered every 3 weeks until the study termination at 10 to 11 weeks postinfection. Control animals received saline infusion at the same time as the rituximab counterparts.

All animals were housed in the University of Pittsburgh Regional Biocontainment Laboratory biosafety level 3 (BSL-3) facility after infection with *M. tuberculosis*. These studies followed all animal experimentation guidelines, and all experimental manipulations and protocols were approved by the University of Pittsburgh School of Medicine Institutional Animal Care and Use Committee.

***M. tuberculosis* infection.** Cynomolgus macaques were infected with a low dose of 4 to 8 CFU of *M. tuberculosis* Erdman strain via intrabronchial instillation as previously described (18, 26). Infection dose was confirmed by plating an aliquot of the *M. tuberculosis* suspension used to infect the animals. Infection was confirmed by conversion of negative to positive tuberculin skin test and elevated peripheral blood mononuclear cell (PBMC) responses to mycobacterial antigens from baseline in lymphocyte proliferation and enzyme-linked immunospot (ELISPOT) assays (19, 26).

Necropsy procedures. All macaques were necropsied at 10 to 11 weeks postinfection. Monkeys were maximally bled prior to necropsy and euthanized using pentobarbital and phenytoin (Beuthanasia; Schering-Plough, Kenilworth, NJ). Gross pathological findings were described by a board-certified veterinary pathologist (E. Klein) and were classified as previously described. Representative sections of each tissue were placed in formalin for histologic analysis or homogenized into single-cell suspensions for immunologic studies, flow cytometric analysis, and bacterial burden, as previously described (18, 19, 26). Bone marrow was also obtained from the sternum as previously described (8). A portion of tissue homogenate from numerous necropsy samples were serially diluted and plated on 7H11 media (BD, Sparks, MD), and CFU were enumerated on day 21, while the rest were filtered using 0.45-μm syringe filter units (Millipore, Darmstadt, Germany) for downstream assays. Total animal CFU count was enumerated by aggregating CFU counts from all lung and lymph node samples. CFU per granuloma counts were calculated by taking into account granuloma size, volume, and specific sample CFU count. CFU data from six of the control animals (17111, 2412, 2512, 20212, 20612, and 20912) were also published in a separate study (27).

Immunologic analysis. Blood was drawn from each animal every 2 weeks starting 2 weeks prior to the first dose of rituximab administration until necropsy at 10 to 11 weeks postinfection. PBMCs were isolated as previously described via Percoll gradient centrifugation (18). Axillary and inguinal lymph nodes were biopsied prior to the first dose of rituximab administration and then at weeks 4 and 8 postinfection.

Flow cytometry. At necropsy, single cell suspensions were derived from lung granulomas, uninvolved lung and thoracic draining lymph nodes. Cells from PBMCs and tissue samples were stained for T cells using anti-human CD3 (clone SP34-2; BD Biosciences), CD4 (clone L200; BD Biosciences), and CD8 (clone DK25; Dako), B cells using anti-human CD20 (clone 2H7; eBioscience) and CD79a (clone HM47; BD Pharmingen), neutrophils with CD11b (clone ICRF44; BD Pharmingen), and calprotectin (clone MAC387; Thermo Scientific) (28) and activation marker HLA-DR (clone LN3; eBioscience). Lymphocytes and neutrophils were identified based on size (forward scatter) and granularity (side scatter). B cells and T cells were further identified based on $CD20^+$ and $CD3^+$ expression, respectively.

For intracellular cytokine staining, tissue single cell suspensions were stimulated in RPMI (Lonza, Walkersville, MD) supplemented with 1% L-glutamine and 1% HEPES (Sigma, St. Louis, MO) containing *M. tuberculosis* CFP10 and ESAT6 peptide pools for T cell stimulation or proteins for B cell stimulation (BEI Resources, Manassas, VA) along with brefeldin A (BD Biosciences), all at a final concentration of 1 μg/ml for 4 h. After staining for CD3, CD4, CD8, and CD20 as described above, the cells were then fixed and permeabilized using BD Cytofix/Cytoperm (BD Biosciences) and finally washed with BD Perm/Wash buffer (BD Biosciences). Cells were then stained with anti-human antibodies against interleukin-2 (IL-2; clone MQ1-17H12; BD Biosciences), IL-6 (clone MQ2-6A3; BD Biosciences), IL-10 (clone JES3-9D7; eBioscience), IL-17 (clone eBio64CAP17; eBioscience), tumor necrosis factor (TNF; clone MAb11; eBioscience), and gamma interferon (IFN-γ; clone B27; BD Biosciences). All cytokine-producing cells were identified as described above.

CD3 percentages obtained by flow cytometry were then used to calculate $CD3^+$ cell numbers on a per-granuloma basis. $CD3^+$ percentages

were not directly reported since B cell depletion would artificially inflate the proportion of $CD3^+$ compartment within the lymphocyte population; thus, only absolute $CD3^+$ counts were used.

Antibody, cytokine, and calprotectin ELISA. *M. tuberculosis*-specific antibodies were quantified via ELISA by coating 96-well plates with 2 μg per well of ESAT6 whole protein or culture filtrate protein (CFP; BEI Resources) dissolved in 1× phosphate-buffered saline (PBS; Lonza). Diluted filtered tissue homogenates were incubated for 1 h at 37°C after blocking for ESAT6 antibody quantification. Serum samples diluted to 1:100 using 1× PBS containing 1% bovine serum albumin were used to assess for anti-rituximab antibodies. Mouse anti-primate IgG conjugated to horseradish peroxidase (clone 1B3; NIH Nonhuman Primate Reagent Resource, Boston, MA) were used as the detection antibody at 1:3,000 dilution. Plates were developed using 3,3′,5,5′-tetramethylbenzidine hydrochloride (Sigma). CFP-specific IgG and total IgG present within tissue homogenates were quantified as previously described (8).

Cytokine enzyme-linked immunosorbent assays (ELISAs) were performed to quantify IL-6, IL-17, TNF, and IL-10. Anti-human IL-10 (Invitrogen, Carlsbad, CA), TNF, IL-6, and anti-primate IL-17 ELISA kits (MabTech, Mariemont, OH) were performed according to the manufacturer's instructions using filtered tissue homogenates obtained at necropsy as samples.

Calprotectin ELISA was performed using the anti-human calprotectin kit (Hycult, Plymouth Meeting, PA) according to the manufacturer's instructions on filtered tissue homogenates obtained at necropsy. The calprotectin ELISA was used as a surrogate marker for neutrophils. All quantifications for cytokine, calprotectin, or antibody amounts were calculated on a per-granuloma basis.

Immunohistochemistry. Tissue sections were embedded with paraffin and stained with hematoxylin and eosin (H&E). These sections were reviewed microscopically by a veterinary pathologist (E. Klein) with specific emphasis on granuloma characteristics as described previously (19). Paraffin-embedded slides of relevant tissue sections were stained as previously described (8) for the presence of T cells (CD3, rabbit polyclonal; Dako, Carpinteria, CA), B cells (CD20, rabbit polyclonal; Neomarkers, Fremont, CA) and antigen-presenting cells (CD11c, clone 5D11, 1:30 dilution; Leica Microsystems, Buffalo Grove, IL). Images were taken at ×20 magnification with an upright confocal laser scanning microscope (Olympus FluoView 500, model BXL21), and serial images were used to generate a composite of the tissue section.

PET/CT scans. PET/CT scans using ^{18}F-labeled fluorodeoxyglucose ($[^{18}F]$FDG) as a probe were performed prior to necropsy in a BSL-3 imaging suite using a hybrid preclinical PET/CT system that includes a micro-PET Focus 220 preclinical PET scanner (Siemens Molecular Solutions, Knoxville, TN) and an eight-slice helical CT scanner (Neurologica Corp., Danvers, MA) as previously described (29).

Data analysis and statistics. Flow cytometry data were analyzed with the FlowJo 9 software package (Tree Star, Ashland, OR). Data were analyzed using Prism 6 (GraphPad Software, San Diego, CA). Medians are shown to account for the variability and skew of the data. The Holm-Sidak method was used to perform multiple *t* tests on the repeated-measures data set, with $P < 0.05$ considered statistically significant. Statistical comparisons were performed using a Mann-Whitney test, with $P < 0.05$ considered statistically significant. The Brown-Forsythe test was used to test the equality of group variances and was performed using JMP 10 (SAS, Cary, NC).

RESULTS

Rituximab depletes B cells of macaques within the blood and tissue compartments. Rituximab was administered 2 weeks prior to *M. tuberculosis* infection to ensure that B cell numbers were minimal upon infection. Subsequent doses of rituximab were given every 3 weeks to ensure sustained B cell depletion over the course of the study (Fig. 1A, black arrows). PBMCs from biweekly blood draws and single cell suspension from monthly peripheral lymph node biopsy specimens were stained with anti-human CD20 and CD79a to identify B cells. CD79a was used as an alternative B cell marker to independently confirm B cell depletion in the event that rituximab interferes with CD20 staining via flow cytometry. Animals given rituximab had almost no B cells in the peripheral blood and significantly reduced frequency of B cells within peripheral lymphoid tissue compared to saline control animals (Fig. 1B). Thus, B cell depletion within peripheral blood and lymphoid compartments was successfully achieved in all eight treated animals with no treatment failures. Some of the macaques did not respond well to repeated rituximab administration. Thus, we curtailed the experiment at 10 to 11 weeks postinfection with *M. tuberculosis* and subsequently were not able to test the effects of longer-term B cell depletion on the infection. Therefore, the results presented here should be interpreted as effects of B cell depletion on early infection only.

At necropsy, single cell suspensions of tissue samples stained with CD20 and CD79a antibodies showed markedly reduced B cell numbers within lung granulomas of rituximab-treated animals (median B cell percentage of live cell gate: rituximab [0.60%] versus saline [3.68%], one to nine samples per animal, $n = 8$ animals per group, Fig. 1C). Thoracic lymph node samples of rituximab-treated animals showed a similar reduction in B cells compared to animals receiving saline (median B cell percentage of live cell gate: rituximab [0.60%] versus saline [13.40%], three to five samples per animal, $n = 8$ animals per group). CD79a staining gave similar results to CD20 staining in lung granuloma and thoracic lymph node samples (Fig. 1D).

Immunohistochemistry staining of lung granulomas from rituximab-treated animals showed substantially reduced numbers and size of B cell aggregates compared to granulomas from saline control animals (Fig. 1E). B cell follicles were similarly reduced within thoracic lymph nodes of rituximab-treated animals compared to control lymph nodes (Fig. 1E). These data in aggregate confirm that rituximab treatment was successful in substantially reducing the peripheral and tissue B cell populations in cynomolgus macaques for the duration of the study.

B cell depletion is accompanied by a reduction in antibody levels within lung and lymphoid tissue. Tissue homogenates prepared from lung granuloma and thoracic lymph node samples were used to quantify *M. tuberculosis* specific IgG and total IgG by ELISA. Lung granulomas of rituximab-treated animals showed significantly smaller amounts of total IgG, as well as IgG specific for the mycobacterial antigens contained in CFP or the ESAT6 protein of *M. tuberculosis* (Fig. 2A), compared to control animals. Similarly, thoracic lymph node samples from rituximab-treated animals had smaller amounts of CFP-specific antibody and total IgG compared to that from saline control animals (ESAT6-specific antibody was not tested in lymph nodes) (Fig. 2B).

In contrast to tissue, levels of circulating CFP-specific antibodies and total IgG in plasma were not significantly different between rituximab-treated and saline control animals (data not shown); the evolution of CFP-specific antibodies was relatively slow in several of the control macaques. A plasma cell ELISPOT assay measuring the number of IgG-producing plasma cells in bone marrow showed that rituximab-treated animals had comparable numbers of IgG plasma cells compared to control animals (Fig. 2C).

Bacterial burden varied substantially in B cell-depleted animals. As noted above, *M. tuberculosis* infection in macaques is

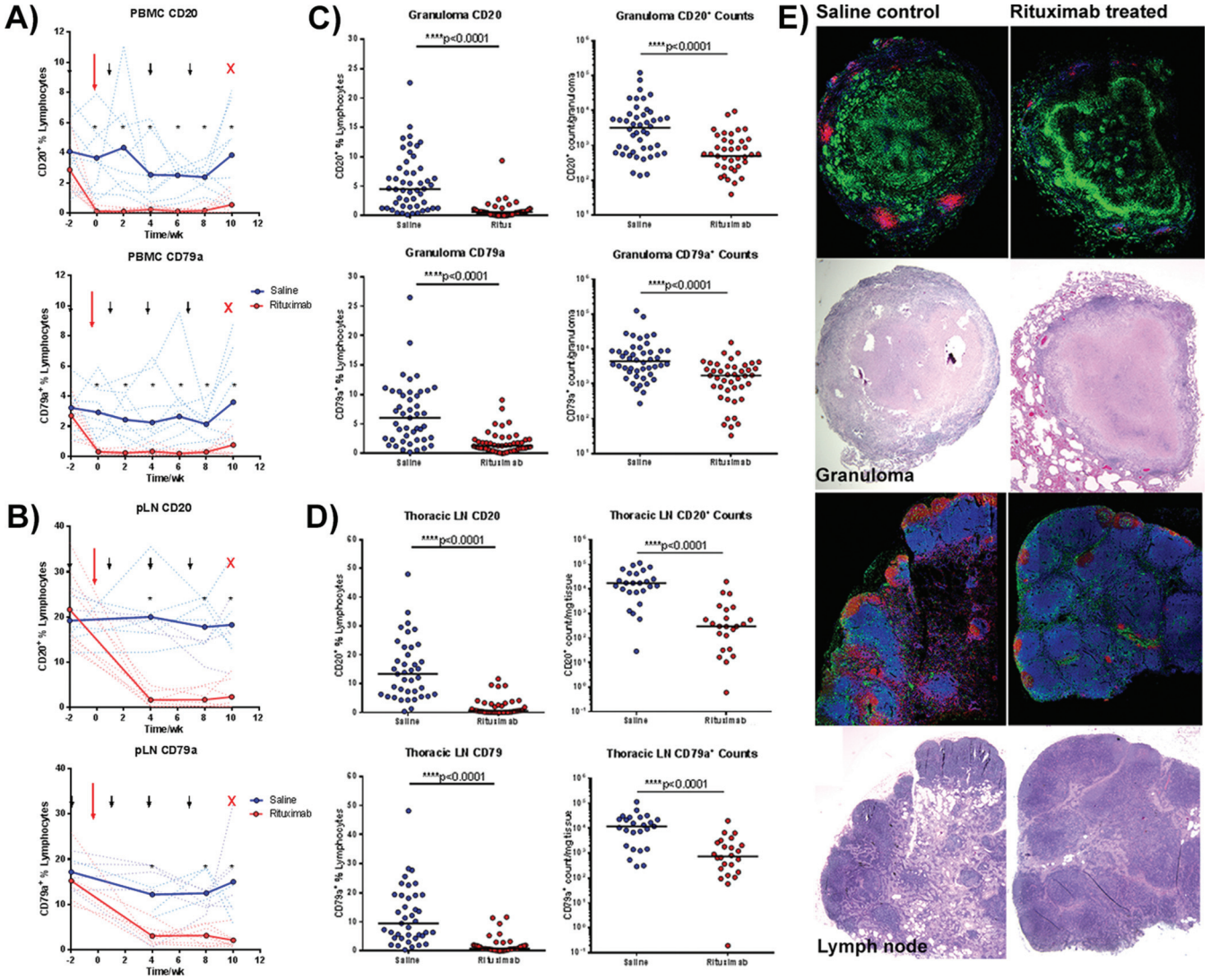

FIG 1 Confirmation of B cell depletion following rituximab treatment. Repeated measures of CD20 and CD79a by fluorescence-activated cell sorting (FACS) within PBMCs (A) and peripheral lymph node (pLN) biopsy specimens (B) to confirm B cell depletion within rituximab-treated animals (red) versus saline-treated controls (blue). Solid lines depict the group average, while dotted lines represent individual animals. Black arrows denote rituximab administration, the large red arrow denotes time of infection, and the red "X" denotes necropsy. $n = 16$ animals, 8 animals per group. An asterisk (*) represents statistical significance for values at the indicated time point with $P < 0.05$ using the Holm-Sidak method. (C) At necropsy, single cell suspensions obtained from granulomas were subjected to FACS staining for CD20 and CD79a quantification. Each point represents one granuloma ($n = 16$ animals, $n = 100$ granulomas, ~6 granulomas per animal). (D) Similar staining to confirm B cell depletion was performed on thoracic LN samples obtained at necropsy. Each point represents one thoracic LN sample ($n = 16$ animas, $n = 78$ thoracic LN samples, ~4 thoracic LN per animal). (E) Immunohistochemistry staining of paraffin-embedded granuloma (top four) and thoracic lymph node samples (bottom four panels) with CD20 (red), CD11b (green), and CD3 (blue) and H&E stains underneath each section confirmed the loss of B cell clusters within rituximab-treated animals. All statistical *P* values were obtained using the Mann-Whitney test unless otherwise stated.

variable across and within individual animals, and analysis can be performed on the overall infection and individual lesions. Prior to necropsy, PET/CT scanning using [^{18}F]FDG was performed to assess disease progression and provide a "roadmap" for harvesting specific lesions at necropsy, as previously described (29). In addition, [^{18}F]FDG avidity is an indirect measure of inflammation (30). Rituximab and saline control animals had similar numbers of lung granulomas observed on PET/CT scan (Fig. 3A). No significant difference was observed in overall [^{18}F]FDG avidity in the lungs of individual animals between the rituximab and saline groups, although, in contrast to the control animals, three animals in the rituximab treatment group had decreased total [^{18}F]FDG avidity relative to untreated macaques, indicating low inflammation (Fig. 3A). Individual granulomas from rituximab-treated animals have modestly but significantly reduced [^{18}F]FDG avidity compared to granulomas from saline control animals (Fig. 3A; $P < 0.005$). Median lung granuloma size, as measured by CT, within rituximab-treated animals were noted to be about 0.5 mm smaller than the saline control median, albeit with a wide range (Fig. 3A).

At necropsy, the gross pathology findings of each animal were used to compile necropsy scores. This score takes into account various pathological findings, including the number of granulomas within each lobe, the extent of lymph node involvement, dis-

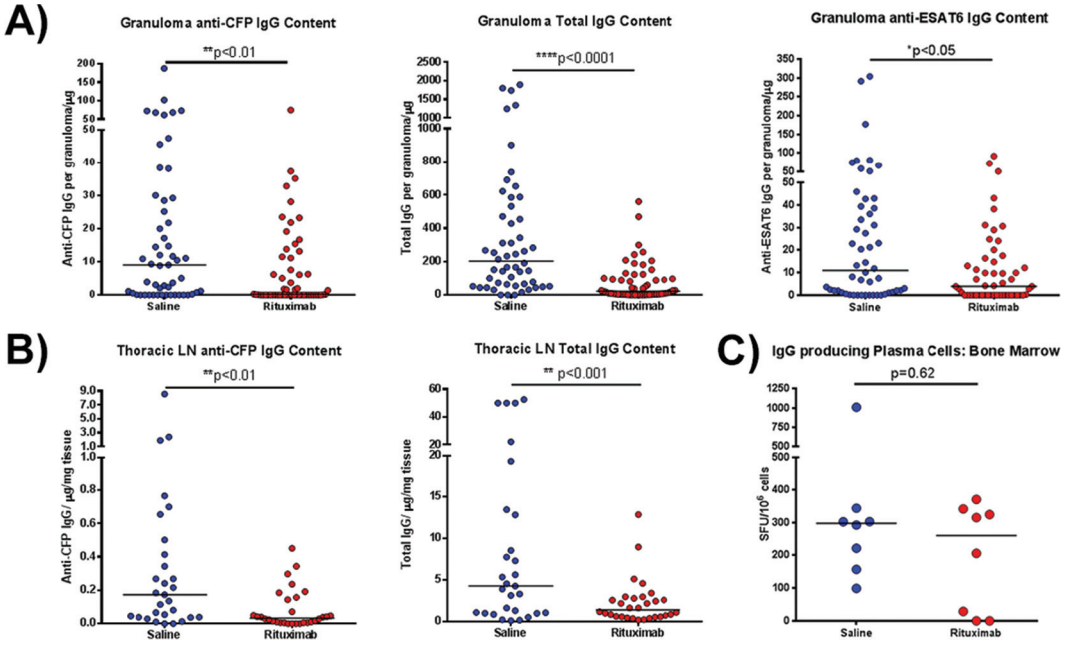

FIG 2 Assessment of antibody profile of granuloma homogenates after rituximab treatment. (A) Granuloma homogenates obtained at necropsy were assayed for the amount of CFP-specific IgG, ESAT6-specific IgG, or total IgG present using ELISA. Antigen-specific IgG levels were significantly reduced after rituximab treatment compared to saline controls (the median granuloma antibody content was reduced ~10-fold in the case of CFP and 5-fold for ESAT6). The total IgG content within rituximab-treated granulomas was also reduced by ~10-fold. Each point represents one granuloma ($n = 16$ animals, $n = 110$ granulomas, ~6 granulomas per animal). (B) Homogenates from lymph node samples were assayed for the amount of CFP-specific IgG and total IgG present. Both antigen specific IgG and total IgG were reduced with rituximab by approximately 2- to 5-fold. Each point represents one thoracic LN sample ($n = 16$ animals, $n = 59$ thoracic LN samples, ~3 thoracic LN samples per animal). (C) The number of plasma cells generating IgG within the bone marrow, assayed by a plasma cell ELISPOT assay, were similar within both groups. Each point presents one animal ($n = 16$ animals, ~8 animals per group). All statistical *P* values were obtained using the Mann-Whitney test unless otherwise stated.

ease dissemination within the lungs, or the presence of extrapulmonary disease (31). A higher number indicates more severe disease. Rituximab-treated animals trended toward lower necropsy scores than the control animals, but the difference was not statistically significant (Fig. 3B).

Bacterial numbers of individual lung granulomas were significantly higher in the rituximab-treated animals than in untreated controls (~5-fold, $P < 0.0001$) (Fig. 3C; middle panel). However, the total bacterial burden, calculated as the sum of CFU derived from all individual lung granulomas, other lung pathologies, and thoracic lymph nodes, was not significantly different between the rituximab-treated and untreated groups (Fig. 3C, left panel, $P = 0.23$). No differences in bacterial burden were observed in thoracic lymph nodes between the groups (Fig. 3C, right panel, $P = 0.67$). Interestingly, rituximab-treated macaques displayed substantially more variation in median lung granuloma CFU among individual monkeys compared to control animals (Fig. 3D). A statistical analysis of CFU/granuloma from B cell-depleted animals versus controls showed that the observed discrepancy in the variation between the rituximab-treated and untreated groups was significantly different (Brown-Forsythe test, $P < 0.0001$), suggesting that depletion of B cells had larger effects in some animals (and some granulomas) than in others. The percentage of sterile lung granulomas or lymph nodes was similar between the groups (Fig. 3E).

Cytokine secretion by granuloma T cells was altered with B cell depletion. We next sought to determine whether the absence of B cells influenced immune responses in the granulomas. Single cell suspensions from individual granulomas obtained at necropsy were analyzed by flow cytometry to assess T cell numbers. The numbers of $CD3^+$ T cells and the percentages of $CD4^+$ or $CD8^+$ T cells in granulomas were not affected by B cell depletion (Fig. 4A). B cells are known to functionally interact with and influence T cells (32); therefore, although the absolute T cell numbers were unchanged, the function of the CD3 population in the rituximab-treated or untreated groups of macaques can be different. Consequently, we investigated the effects of B cell depletion on the following granuloma T cell cytokines that can modulate the local immune environment of granulomas during *M. tuberculosis* infection: IL-17, which plays an important role in neutrophil recruitment; TNF and IFN-γ, the signature of a T_H1 response and critical for macrophage activation; IL-2, which promotes T cell proliferation; and IL-10, a major immunoregulatory cytokine. Granuloma samples were stimulated with immunodominant *M. tuberculosis* antigens ESAT6 and CFP10 peptide pools and cytokine expression assessed using intracellular cytokine staining and flow cytometry (Fig. 4B and see Fig. S1 in the supplemental material). The frequency of T cells secreting IFN-γ or TNF was similar in granulomas from rituximab- or saline-treated animals. However, granulomas from rituximab-treated macaques had a higher frequency of $CD3^+$ cells producing IL-17, IL-2, or IL-10 than those from control animals (Fig. 4B). When stratified according to individual animals, the increase in IL-17, IL-2, or IL-10 positive CD3 percentages were not equally distributed across all animals, highlighting the variation in granulomas within a single animal and

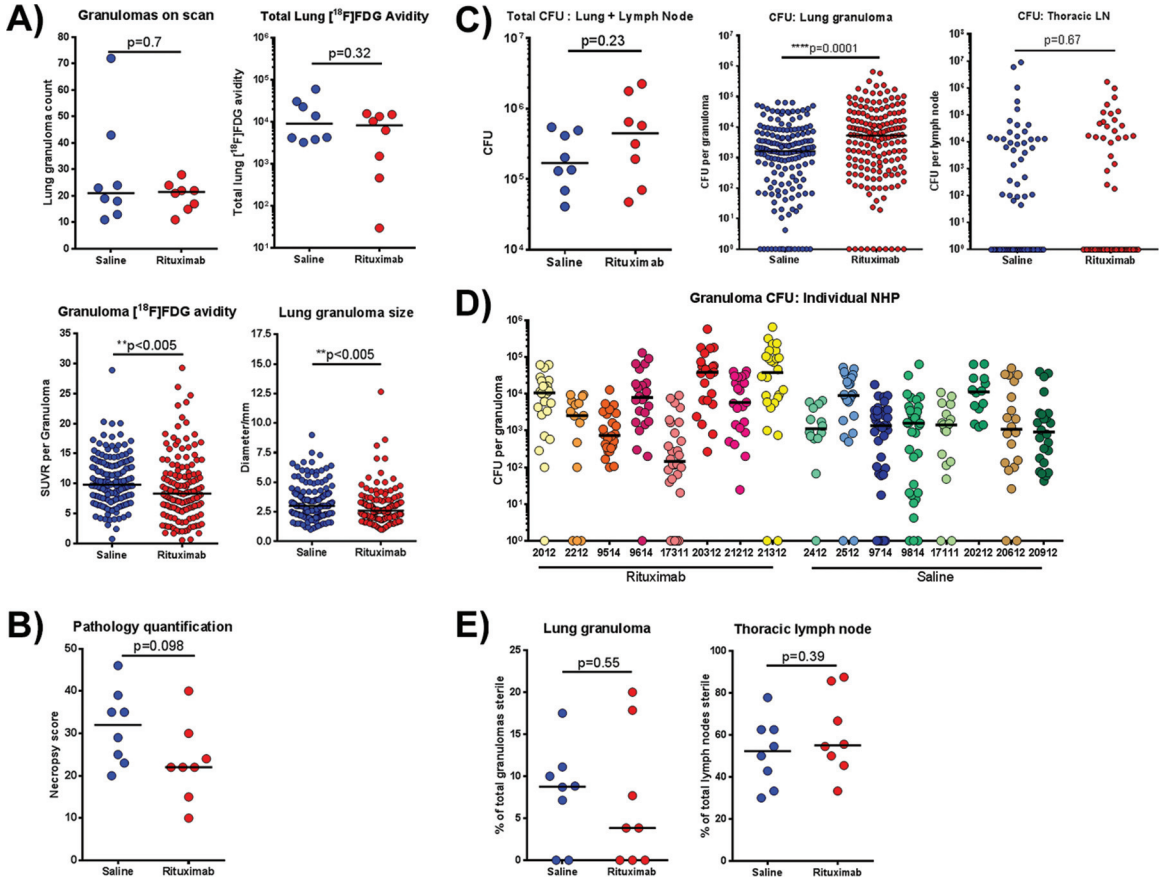

FIG 3 Clinical and pathology findings for animals at necropsy. (A) PET/CT scans were conducted prior to necropsy using [^{18}F]FDG to identify and characterize granulomas. Within both groups, similar granuloma numbers were identified on scans, and the overall lung [^{18}F]FDG avidities were comparable. Each symbol is an animal (n = 16 animals, 8 animals per group). The granuloma [^{18}F]FDG avidity (standard uptake value [SUV]), although statistically significant, was only marginally lower in the rituximab-treated group. The sizes of granulomas were determined using CT. Each symbol is a granuloma (n = 319 granulomas, ~19 granulomas per animal). (B) Gross pathology scores at necropsy. (C) Tissue sample homogenates obtained at necropsy were plated on 7H11 agar to enumerate the bacterial CFU. The total bacterial burden refers to the absolute number of CFU present within the thoracic cavity of each animal; each symbol is one animal (n = 16 animals). CFU counts from individual lung granulomas were then compared between both groups; each point represents one granuloma (n = 319 granulomas, ~19 granulomas per animal). CFU counts from thoracic LN samples were comparable between both groups. Each point represents one thoracic LN sample (n = 138 samples, ~9 lymph nodes per animal). (D) Granuloma CFU counts were further stratified according to individual animals. Each symbol is a single granuloma, and each individual monkey ID is on the x axis. Median CFU values per granuloma for the control group animals were ~10^3 bacteria with some variability. However, variability within rituximab animals was much larger, with a higher distribution between animals within the group. A Brown-Forsythe test was used to establish that the observed difference in variability between both groups were statistically significant ($P < 0.0001$). (E) The capacity of granulomas and lymph nodes to sterilize bacteria was also assessed by comparing the number of granulomas with no recoverable CFU. Each symbol represents an animal (n = 16 animals, 8 animals per group). All statistical P values were obtained using the Mann-Whitney test unless otherwise stated.

across animals within the group (see Fig. S2 in the supplemental material).

B cell depletion alters cytokine levels in granulomas. It is known that B cell cytokines can regulate T cell functions (33). Thus, the higher levels of lung granuloma CD3$^+$ cells producing IL-17, IL-2, and IL-10 observed in the rituximab-treated macaques (Fig. 4B) could be caused by the absence of certain B cell cytokines as a result of B cell depletion. We therefore assessed the array of cytokines produced by granulomatous B cells during *M. tuberculosis* infection. Intracellular cytokine staining of granuloma-derived cells from saline control (non-B cell-depleted) infected animals was performed after stimulation with whole ESAT6 and CFP10 proteins. B cells from granulomas in *M. tuberculosis*-infected macaques predominantly secreted IL-6 or IL-17 (median of 12% of B cells for either cytokine) and, to a lesser extent, IL-10 and IFN-γ. Very few B cells within the granuloma were noted to make IL-2 or TNF (Fig. 5A). These data reinforce the notion that B cells can produce a range of cytokines that can modulate an immunological environment (23, 34).

Cytokines can also be produced by cells other than B or T cells in tuberculous granulomas, including macrophages, the dominant cell in granulomas (35). Data from mouse TB models indicated massive neutrophil influx into the lungs and elevated IL-10 in the absence of B cells, suggesting possible defects in inflammation control in B cell-deficient animals (4, 13). To obtain a more complete picture of the cytokine environment in granulomas, ELISAs were performed on granuloma homogenates to assess the levels of proinflammatory cytokines IL-6, IL-17, and TNF, and for calprotectin, a marker for neutrophils (28). Granulomas from rituximab-treated animals had reduced amounts of IL-6 and IL-10 compared to those from control animals, but the IL-17 and TNF levels were not statistically different between the

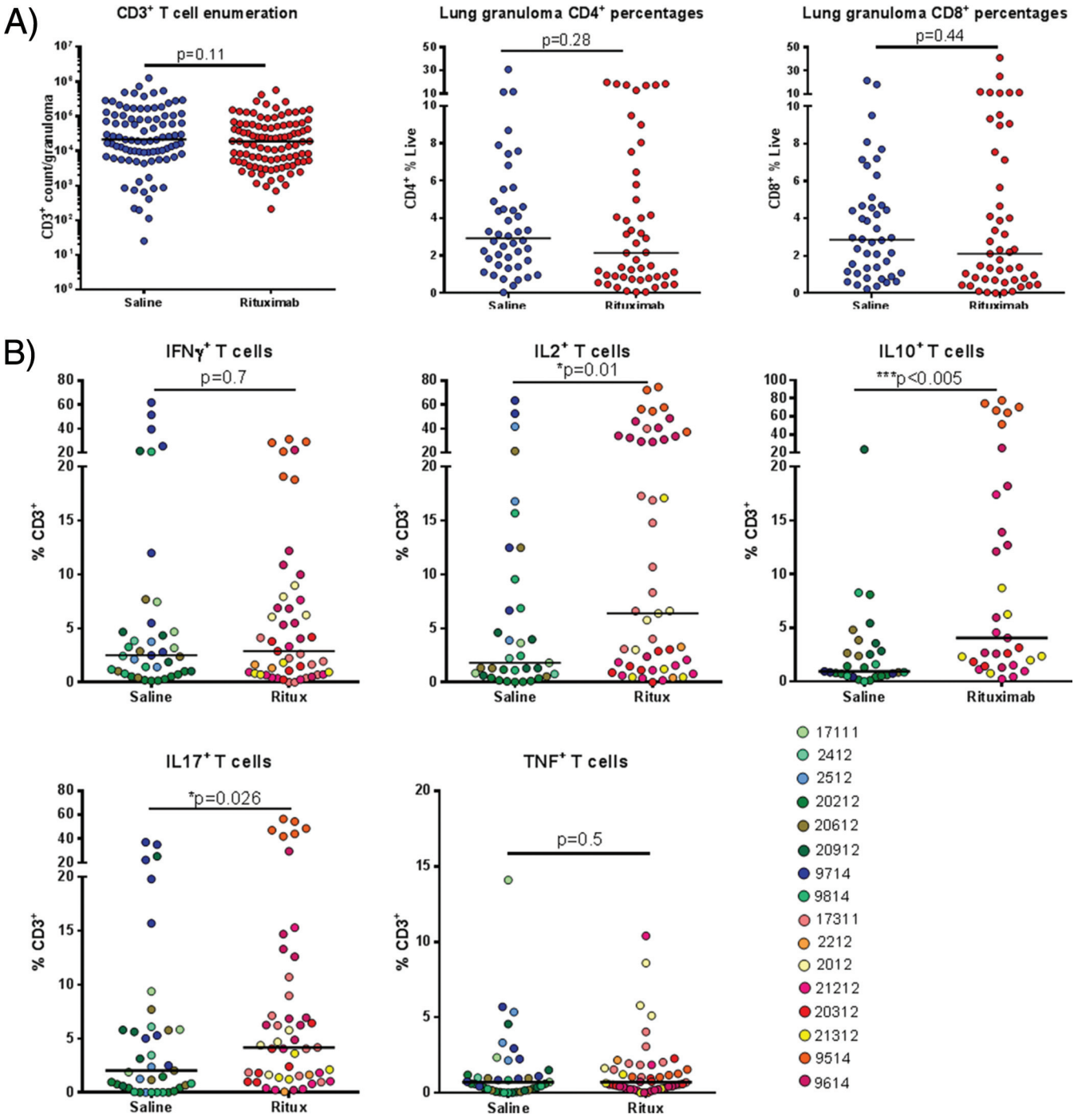

FIG 4 Effects of B cell depletion on T cell populations within the granuloma. (A) Single cell suspensions from granulomas were analyzed by FACS to identify T cells via CD3, CD4, and CD8 markers. Each symbol represents one granuloma. For CD3 enumeration, $n = 16$ animals and $n = 191$ granulomas, and thus there were ~11 granulomas per animal. For CD4 and CD8 analysis, $n = 16$ animals and $n = 93$ granulomas, and thus there were ~5 granulomas per animal. (B) The CD3 population were analyzed for cytokine production using intracellular cytokine staining via FACS, specifically IL-17, IL-2, IL-10, IFN-γ, and TNF. Each symbol represents a granuloma, and the colors differentiate granulomas from individual animals ($n = 16$ animals, $n = 87$ granulomas, ~5 granulomas per animal for IL-17, IL-2, IFN-γ, and TNF). For IL-10, $n = 10$ animals and $n = 62$ granulomas, and thus there were ~6 granulomas per animal. All statistical *P* values were obtained using the Mann-Whitney test.

groups (Fig. 5B). The difference in the cytokine profiles of whole lung granulomas and that of granuloma T cells suggest the regulation of the cytokine network in tuberculous granulomas of *M. tuberculosis*-infected macaques is complex. Calprotectin protein levels were also similar between rituximab-treated and control granulomas, suggesting similar levels of neutrophils (Fig. 5C), a finding consistent with histological analysis (data not shown).

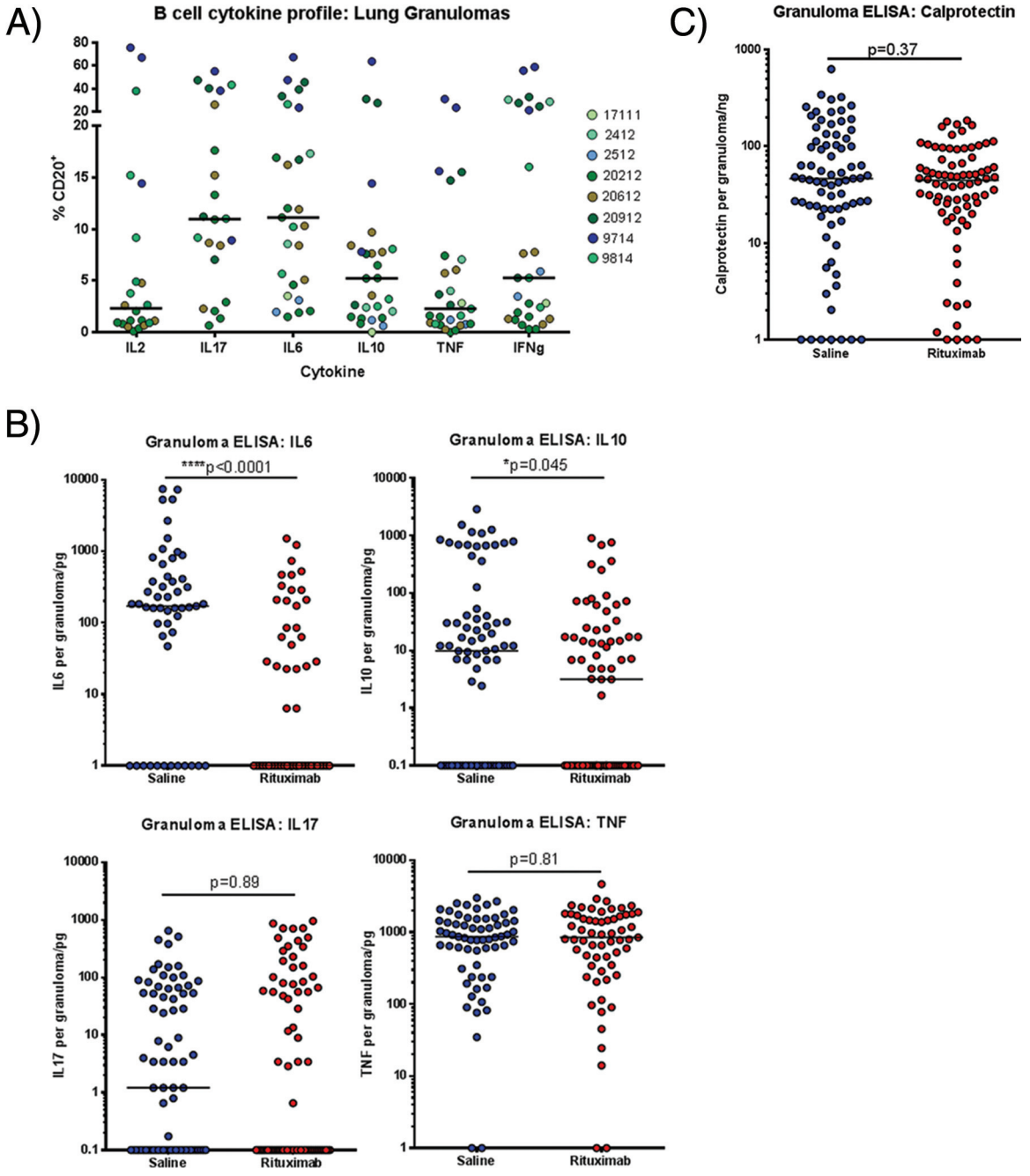

FIG 5 Effects of B cell depletion on granuloma cytokine and neutrophil profiles. (A) Single cell suspensions from saline control granulomas were stained for B cell markers and cytokine antibodies to determine the cytokine secretion profile of B cells via intracellular FACS. Six cytokines were selected to be assayed: IL-2, IL-6, IL-10, IL-17, TNF, and IFN-γ. Each symbol is a granuloma, and colors denote granulomas from individual animals. For IL-6, IL-10, TNF, and IFN-γ, n = 8 animals and n = 27 granulomas, and thus there were ~4 granulomas per animal. For IL-2 and IL-17, n = 5 animals and n = 22 granulomas, and thus there were ~4 granulomas per animal. (B) ELISAs to quantify cytokine amounts were performed on granuloma homogenates for four cytokines, IL-6, IL-10, IL-17, and TNF to determine whether B cell depletion via rituximab perturbed the cytokine balance within the granulomas. Each symbol is a granuloma (n = 16 animals, n = 136 granulomas, ~8 granulomas per animal). (C) Neutrophil amounts were quantified based on the amount of calprotectin present within granuloma homogenates. Each symbol is a granuloma (n = 16 animals, n = 155 granulomas, ~10 granulomas per animal). All statistical P values were obtained using the Mann-Whitney test.

DISCUSSION

The goal of this study was to determine whether B cell depletion affects the outcome of *M. tuberculosis* infection in nonhuman primates. How B cells affect tuberculosis immunity has only been studied in mice, where B cells and humoral immunity are necessary for the development of optimal anti-TB immunity and for restricting excessive inflammation in the acute phase of infection (4, 11–16). In contrast, it has been reported that lung inflamma-

tion during chronic TB in B cell-deficient $\mu MT^{-/-}$ mice infected with either *M. tuberculosis* CDC1551 (17) or Erdman (J. Chan et al., unpublished data) was attenuated compared to wild-type mice. These data suggest that B cells regulate the lung granulomatous response in an infection phase-specific manner. In the present study, we show that while rituximab treatment did not significantly affect the overall pathology, disease progression, or clinical outcome in *M. tuberculosis*-infected macaques, the results derived from detailed analysis of individual lung granulomas indicate that B cells can significantly modulate cytokine production, bacterial burden, and inflammation levels in these lesions. The data also demonstrate that B cell cytokine production within granulomas is highly variable, even among individual granulomas from the same animal. This observation is similar to our previous macaque data that bacterial burden, macrophages, and T cell responses are variable among granulomas, even within the same animal (27, 35, 36). These data suggest a role for B cells in controlling infection in at least a subset of granulomas or animals, underscoring the variability of the immunologic environment among granulomas within the lung of an individual monkey. Since the 10- to 11-week time point postinfection represents the bridge between early and chronic infection in macaques, the variability in the B cell-depleted animals may reflect the dichotomous effects of B cells in early versus late infection, as has been observed in the murine system (17; Chan et al., unpublished), further compounding the complexity of intergranuloma variation. Because this study only examined B cell depletion during early infection, we do not know what the longer term effects of B cell depletion would be on disease progression in chronic infection.

Rituximab treatment greatly reduced B cells and antibody production at the sites of infection, both in lung granulomas and in thoracic lymph nodes. The reduction in both antigen-specific and total IgG levels within infected tissues could be due to the reduction or loss of B cell clusters. The direct effect of antibody depletion locally at the sites of infection is unknown, although antibody binding has been shown to enhance bacillus uptake and killing by macrophages by activating FcγR engagement (37). Macrophage activation is also known to be influenced by the size of immune complexes, with both pro- and anti-inflammatory outcomes being possible (38). Data on murine FcγR in the context of TB support that FcγR can affect the control of disease (14). However, a limitation in macaques is that the effects of antibody mediated pathways of disease control cannot be untangled from B cell depletion, making it difficult to attribute direct actions of antibody in disease control in addition to cytokine signaling. Antibodies that distinguish the activating and inhibiting FcγRs in macaques are not currently available, which prohibits the study of how FcγR influences macrophage activation within the granuloma of nonhuman primates.

At necropsy, gross pathology, clinical disease manifestation, and progression were similar when comparing B cell-depleted animals to the saline control counterparts. The most intriguing observations were the increase in median CFU on a per-granuloma basis (~5-fold) from B cell-depleted lung granulomas and the wider variation in median CFU per granuloma from individual animals. This indicates that B cell depletion affected the efficacy of local disease control, at least in some granulomas and some animals. B cells are known to interact with macrophages and T cells (14, 21, 32, 39, 40) and can affect differential macrophage activation states and T helper cell polarization depending on antigen presentation or cytokine secretion. B cell and macrophage interaction is further complicated by Fc receptor engagement, which can further modulate pro- or anti-inflammatory reactions (38, 41). As a result, the B cells can potentially modulate the local environment of tuberculous granulomas via a range of pathways.

B cell clusters within the lung granulomas were previously characterized as being areas where antigen presentation occurs judging from the increased expression of major histocompatibility complex class II molecules and the proliferation of B cells (8). The absence of such clusters within the granulomas and reduced B cell follicles within the lymph nodes may thus reduce the efficacy of proliferation, activation, differentiation, and trafficking of antigen-specific T cells into the granuloma (33). We noted significant changes in cytokine production by T cells within lung granulomas upon B cell depletion, with an increase in IL-2, IL-10, and IL-17 producing T cells within rituximab-treated macaques. IL-2 is associated with a wide range of T cell functions such as proliferation, particularly among the CD8 and regulatory T cell populations (42, 43). It is possible that the increase in IL-2-secreting T cells may be an attempt to boost T cell numbers given the higher bacterial burden within B cell-depleted granulomas. IL-2 is also crucial in the development of regulatory T cells (44, 45). More regulatory T cells can be beneficial by reducing bystander damage via T cell suppression within granulomas but, conversely, can also be detrimental toward disease control by inhibiting immune activation locally within the granuloma site (46). Although we did not specifically assess Tregs in this study, the alteration in T cell cytokine secretion, particularly IL-2 and IL-10, suggests that regulatory T cells may be increased in B cell-depleted granulomas. An oversuppression of the immune system would, in turn, allow *M. tuberculosis* to proliferate more, leading to the increase of overall CFU within a subset of B cell-depleted granulomas.

Higher numbers of T cells producing IL-17 within rituximab-treated granulomas can be beneficial for bacterial control since IL-17 production has been linked to increased IFN-γ-secreting T cell recruitment (47). IL-17 signaling can also result in an influx of neutrophils into the granuloma. However, despite noting an increase of IL-17-secreting T cells, this study did not observe any increases in IFN-γ production or neutrophil recruitment. Thus, the significance of increased TH-17 cells in a subset of B cell-depleted granulomas is not clear at this time.

When measuring overall cytokine content, IL-6 and IL-10 levels were decreased within B cell-depleted granulomas. B cells were noted to secrete primarily IL-6 and IL-10 in granulomas from control animals and global reductions of these cytokines within the granulomas of rituximab-treated macaques could be attributed to B cell depletion. Indeed, B cells are prodigious producers of IL-6 in other immune settings, such as multiple sclerosis (48). IL-6 has multiple roles in inflammation, particularly B cell expansion (34, 48) and T cell development (49). A decrease in IL-6 suggests that the inflammatory response within the B cell-depleted granuloma may be less robust compared to control granulomas since IL-6 is involved in coordinating immune cell recruitment, particularly neutrophils and T cells during the acute phase of infection (50, 51). The lower [^{18}F]FDG avidity of individual granulomas (by PET imaging) supports this notion. Without proper cell recruitment, B cell-depleted granulomas may not be able to efficiently exert antimycobacterial effects, which may contribute to the higher observed bacterial burden.

This study shows that B cell depletion did not significantly alter

the overall acute *M. tuberculosis* progression and outcome in infected macaques, at least up to 10 weeks. However, data obtained from detailed analysis of individual granulomas showed that B cells clearly contribute to modulation of immune responses, as assessed by the level of cytokine production and inflammation and by the bacterial burden in the lesions. These data provide insights into local B cell responses during *M. tuberculosis* infection, which could potentially be targeted to enhance the efficacy of a therapeutic strategy. The data also demonstrate that these immunologic parameters vary among individual granulomas, suggesting a differential effect of B cells in different granulomas and in different monkeys, and this could at least be partially attributed to the previously reported heterogeneity of granulomas in *M. tuberculosis*-infected macaques (27, 29, 36). The observed intergranuloma variety can be further augmented by the endpoint of the study (~10 weeks postinfection), which coincides with the period during which the infection is transitioning from the acute to the chronic phase, when the potential differential phase-dependent functions of B cells, as suggested in mouse studies (17; Chan et al., unpublished), can manifested. It is possible, based on the multiple effects of rituximab treatment on the local granulomatous response, including cytokine production, inflammation levels ,and bacterial burden, that longer-term depletion of B cells would result in more exaggerated differences in infection outcome. The performance of such studies, which are challenging with antibody administration in the present model, must await the development of novel means of manipulating B cells and humoral immunity in nonhuman primates.

ACKNOWLEDGMENTS

The primate reagents used in these studies were provided by the Nonhuman Primate Reagent Resource funded by NIAID contract HHSN2722000130031C, directed by Keith Reimann (Beth Israel Deaconess Medical Center, Harvard University, now the University of Massachusetts Medical School), who also provided valuable advice in conducting the studies. We gratefully acknowledge Edwin Klein and Chris Janssen for performing necropsy and histologic analyses and the technical assistance provided by Mark Rodgers, Catherine Cochran, Melanie O'Malley, Jamie Tomko, Dan Filmore, Carolyn Bigbee, Chelsea Chedrick, and Paul Johnston. We also appreciate the guidance from Jorn Schmitz (Harvard Medical School) regarding use of rituximab in macaques.

This study was supported by the Bill and Melinda Gates Foundation and NIH RO1 HL68526 (J.C. and J.L.F.) and RO1 HL075845 (J.L.F.). The funders had no role in study design, data collection and interpretation, or the decision to submit the work for publication.

FUNDING INFORMATION

This work, including the efforts of Jiayao Phuah, John Chan, Philana Ling Lin, and JoAnne L. Flynn, was funded by HHS | National Institutes of Health (NIH) (HL68526). This work, including the efforts of Hannah Gideon, Philana Ling Lin, and JoAnne L. Flynn, was funded by HHS | National Institutes of Health (NIH) (HL075845). This work, including the efforts of Hannah Gideon, Pauline Maiello, M. Teresa Coleman, Philana Ling Lin, and JoAnne L. Flynn, was funded by Bill and Melinda Gates Foundation.

REFERENCES

1. **Chan J, Mehta S, Bharrhan S, Chen Y, Achkar JM, Casadevall A, Flynn J.** 2014. The role of B cells and humoral immunity in *Mycobacterium tuberculosis* infection. Semin Immunol **26:**588–600. http://dx.doi.org/10.1016/j.smim.2014.10.005.
2. **Slight SR, Rangel-Moreno J, Gopal R, Lin Y, Fallert Junecko BA, Mehra S, Selman M, Becerril-Villanueva E, Baquera-Heredia J, Pavon L, Kaushal D, Reinhart TA, Randall TD, Khader SA.** 2013. CXCR5$^+$ T helper cells mediate protective immunity against tuberculosis. J Clin Invest **123:**712–726. http://dx.doi.org/10.1172/JCI65728.
3. **Tsai MC, Chakravarty S, Zhu G, Xu J, Tanaka K, Koch C, Tufariello J, Flynn J, Chan J.** 2006. Characterization of the tuberculous granuloma in murine and human lungs: cellular composition and relative tissue oxygen tension. Cell Microbiol **8:**218–232. http://dx.doi.org/10.1111/j.1462-5822.2005.00612.x.
4. **Maglione PJ, Xu J, Chan J.** 2007. B cells moderate inflammatory progression and enhance bacterial containment upon pulmonary challenge with *Mycobacterium tuberculosis*. J Immunol **178:**7222–7234. http://dx.doi.org/10.4049/jimmunol.178.11.7222.
5. **Gonzalez-Juarrero M, Turner OC, Turner J, Marietta P, Brooks JV, Orme IM.** 2001. Temporal and spatial arrangement of lymphocytes within lung granulomas induced by aerosol infection with *Mycobacterium tuberculosis*. Infect Immun **69:**1722–1728. http://dx.doi.org/10.1128/IAI.69.3.1722-1728.2001.
6. **Turner J, Frank AA, Brooks JV, Gonzalez-Juarrero M, Orme IM.** 2001. The progression of chronic tuberculosis in the mouse does not require the participation of B lymphocytes or interleukin-4. Exp Gerontol **36:**537–545. http://dx.doi.org/10.1016/S0531-5565(00)00257-6.
7. **Khader SA, Rangel-Moreno J, Fountain JJ, Martino CA, Reiley WW, Pearl JE, Winslow GM, Woodland DL, Randall TD, Cooper AM.** 2009. In a murine tuberculosis model, the absence of homeostatic chemokines delays granuloma formation and protective immunity. J Immunol **183:**8004–8014. http://dx.doi.org/10.4049/jimmunol.0901937.
8. **Phuah JY, Mattila JT, Lin PL, Flynn JL.** 2012. Activated B cells in the granulomas of nonhuman primates infected with *Mycobacterium tuberculosis*. Am J Pathol **181:**508–514. http://dx.doi.org/10.1016/j.ajpath.2012.05.009.
9. **Ulrichs T, Kosmiadi GA, Jorg S, Pradl L, Titukhina M, Mishenko V, Gushina N, Kaufmann SH.** 2005. Differential organization of the local immune response in patients with active cavitary tuberculosis or with nonprogressive tuberculoma. J Infect Dis **192:**89–97. http://dx.doi.org/10.1086/430621.
10. **Ulrichs T, Kosmiadi GA, Trusov V, Jorg S, Pradl L, Titukhina M, Mishenko V, Gushina N, Kaufmann SH.** 2004. Human tuberculous granulomas induce peripheral lymphoid follicle-like structures to orchestrate local host defence in the lung. J Pathol **204:**217–228. http://dx.doi.org/10.1002/path.1628.
11. **Vordermeier HM, Venkataprasad N, Harris DP, Ivanyi J.** 1996. Increase of tuberculous infection in the organs of B cell-deficient mice. Clin Exp Immunol **106:**312–316. http://dx.doi.org/10.1046/j.1365-2249.1996.d01-845.x.
12. **Bosio CM, Gardner D, Elkins KL.** 2000. Infection of B cell-deficient mice with CDC1551, a clinical isolate of *Mycobacterium tuberculosis*: delay in dissemination and development of lung pathology. J Immunol **164:**6417–6425. http://dx.doi.org/10.4049/jimmunol.164.12.6417.
13. **Kozakiewicz L, Chen Y, Xu J, Wang Y, Dunussi-Joannopoulos K, Ou Q, Flynn JL, Porcelli SA, Jacobs WR, Jr., Chan J.** 2013. B cells regulate neutrophilia during *Mycobacterium tuberculosis* infection and BCG vaccination by modulating the interleukin-17 response. PLoS Pathog **9:**e1003472. http://dx.doi.org/10.1371/journal.ppat.1003472.
14. **Maglione PJ, Xu J, Casadevall A, Chan J.** 2008. Fc gamma receptors regulate immune activation and susceptibility during *Mycobacterium tuberculosis* infection. J Immunol **180:**3329–3338. http://dx.doi.org/10.4049/jimmunol.180.5.3329.
15. **Torrado E, Fountain JJ, Robinson RT, Martino CA, Pearl JE, Rangel-Moreno J, Tighe M, Dunn R, Cooper AM.** 2013. Differential and site specific impact of B cells in the protective immune response to *Mycobacterium tuberculosis* in the mouse. PLoS One **8:**e61681. http://dx.doi.org/10.1371/journal.pone.0061681.
16. **Maglione PJ, Chan J.** 2009. How B cells shape the immune response against *Mycobacterium tuberculosis*. Eur J Immunol **39:**676–686. http://dx.doi.org/10.1002/eji.200839148.
17. **Teitelbaum R, Glatman-Freedman A, Chen B, Robbins JB, Unanue E, Casadevall A, Bloom BR.** 1998. An MAb recognizing a surface antigen of *Mycobacterium tuberculosis* enhances host survival. Proc Natl Acad Sci U S A **95:**15688–15693. http://dx.doi.org/10.1073/pnas.95.26.15688.
18. **Capuano SV, III, Croix DA, Pawar S, Zinovik A, Myers A, Lin PL, Bissel S, Fuhrman C, Klein E, Flynn JL.** 2003. Experimental *Mycobacterium tuberculosis* infection of cynomolgus macaques closely resembles the var-

ious manifestations of human *M. tuberculosis* infection. Infect Immun **71:**5831–5844. http://dx.doi.org/10.1128/IAI.71.10.5831-5844.2003.
19. **Lin PL, Pawar S, Myers A, Pegu A, Fuhrman C, Reinhart TA, Capuano SV, Klein E, Flynn JL.** 2006. Early events in *Mycobacterium tuberculosis* infection in cynomolgus macaques. Infect Immun **74:**3790–3803. http://dx.doi.org/10.1128/IAI.00064-06.
20. **Tasca S, Zhuang K, Gettie A, Knight H, Blanchard J, Westmoreland S, Cheng-Mayer C.** 2011. Effect of B-cell depletion on coreceptor switching in R5 simian-human immunodeficiency virus infection of rhesus macaques. J Virol **85:**3086–3094. http://dx.doi.org/10.1128/JVI.02150-10.
21. **Monson NL, Cravens P, Hussain R, Harp CT, Cummings M, de Pilar Martin M, Ben LH, Do J, Lyons JA, Lovette-Racke A, Cross AH, Racke MK, Stuve O, Shlomchik M, Eagar TN.** 2011. Rituximab therapy reduces organ-specific T cell responses and ameliorates experimental autoimmune encephalomyelitis. PLoS One **6:**e17103. http://dx.doi.org/10.1371/journal.pone.0017103.
22. **Cerny T, Borisch B, Introna M, Johnson P, Rose AL.** 2002. Mechanism of action of rituximab. Anticancer Drugs **13**(Suppl 2):S3–S10. http://dx.doi.org/10.1097/00001813-200211002-00002.
23. **Clatworthy MR.** 2011. Targeting B cells and antibody in transplantation. Am J Transplant **11:**1359–1367. http://dx.doi.org/10.1111/j.1600-6143.2011.03554.x.
24. **Zahn RC, Rett MD, Li M, Tang H, Korioth-Schmitz B, Balachandran H, White R, Pryputniewicz S, Letvin NL, Kaur A, Montefiori DC, Carville A, Hirsch VM, Allan JS, Schmitz JE.** 2010. Suppression of adaptive immune responses during primary SIV infection of sabaeus African green monkeys delays partial containment of viremia but does not induce disease. Blood **115:**3070–3078. http://dx.doi.org/10.1182/blood-2009-10-245225.
25. **Gaufin T, Pattison M, Gautam R, Stoulig C, Dufour J, MacFarland J, Mandell D, Tatum C, Marx MH, Ribeiro RM, Montefiori D, Apetrei C, Pandrea I.** 2009. Effect of B-cell depletion on viral replication and clinical outcome of simian immunodeficiency virus infection in a natural host. J Virol **83:**10347–10357. http://dx.doi.org/10.1128/JVI.00880-09.
26. **Flynn JL, Capuano SV, Croix D, Pawar S, Myers A, Zinovik A, Klein E.** 2003. Non-human primates: a model for tuberculosis research. Tuberculosis **83:**116–118. http://dx.doi.org/10.1016/S1472-9792(02)00059-8.
27. **Gideon HP, Phuah J, Myers AJ, Bryson BD, Rodgers MA, Coleman MT, Maiello P, Rutledge T, Marino S, Fortune SM, Kirschner DE, Lin PL, Flynn JL.** 2015. Variability in tuberculosis granuloma T cell responses exists, but a balance of pro- and anti-inflammatory cytokines is associated with sterilization. PLoS Pathog **11:**e1004603. http://dx.doi.org/10.1371/journal.ppat.1004603.
28. **Mattila JT, Maiello P, Sun T, Via LE, Flynn JL.** 2015. Granzyme B-expressing neutrophils correlate with bacterial load in granulomas from *Mycobacterium tuberculosis*-infected cynomolgus macaques. Cell Microbiol **17:**1085–1097. http://dx.doi.org/10.1111/cmi.12428.
29. **Lin PL, Coleman T, Carney JP, Lopresti BJ, Tomko J, Fillmore D, Dartois V, Scanga C, Frye LJ, Janssen C, Klein E, Barry CE 3rd, Flynn JL.** 2013. Radiologic responses in cynomolgus macaques for assessing tuberculosis chemotherapy regimens. Antimicrob Agents Chemother http://dx.doi.org/10.1128/AAC.00277-13.
30. **Palmer WE, Rosenthal DI, Schoenberg OI, Fischman AJ, Simon LS, Rubin RH, Polisson RP.** 1995. Quantification of inflammation in the wrist with gadolinium-enhanced MR imaging and PET with 2-[F-18]-fluoro-2-deoxy-D-glucose. Radiology **196:**647–655. http://dx.doi.org/10.1148/radiology.196.3.7644624.
31. **Lin PL, Rodgers M, Smith L, Bigbee M, Myers A, Bigbee C, Chiosea I, Capuano SV, Fuhrman C, Klein E, Flynn JL.** 2009. Quantitative comparison of active and latent tuberculosis in the cynomolgus macaque model. Infect Immun **77:**4631–4642. http://dx.doi.org/10.1128/IAI.00592-09.
32. **Parker DC.** 1993. T cell-dependent B cell activation. Annu Rev Immunol **11:**331–360. http://dx.doi.org/10.1146/annurev.iy.11.040193.001555.
33. **Kleindienst P, Brocker T.** 2005. Concerted antigen presentation by dendritic cells and B cells is necessary for optimal CD4 T-cell immunity in vivo. Immunology **115:**556–564. http://dx.doi.org/10.1111/j.1365-2567.2005.02196.x.
34. **Barr TA, Shen P, Brown S, Lampropoulou V, Roch T, Lawrie S, Fan B, O'Connor RA, Anderton SM, Bar-Or A, Fillatreau S, Gray D.** 2012. B cell depletion therapy ameliorates autoimmune disease through ablation of IL-6-producing B cells. J Exp Med **209:**1001–1010. http://dx.doi.org/10.1084/jem.20111675.
35. **Mattila JT, Ojo OO, Kepka-Lenhart D, Marino S, Kim JH, Eum SY, Via LE, Barry CE 3rd, Klein E, Kirschner DE, Morris SM, Jr, Lin PL, Flynn JL.** 2013. Microenvironments in tuberculous granulomas are delineated by distinct populations of macrophage subsets and expression of nitric oxide synthase and arginase isoforms. J Immunol **191:**773–784. http://dx.doi.org/10.4049/jimmunol.1300113.
36. **Lin PL, Ford CB, Coleman MT, Myers AJ, Gawande R, Ioerger T, Sacchettini J, Fortune SM, Flynn JL.** 2014. Sterilization of granulomas is common in active and latent tuberculosis despite within-host variability in bacterial killing. Nat Med **20:**75–79. http://dx.doi.org/10.1038/nm.3412.
37. **de Valliere S, Abate G, Blazevic A, Heuertz RM, Hoft DF.** 2005. Enhancement of innate and cell-mediated immunity by antimycobacterial antibodies. Infect Immun **73:**6711–6720. http://dx.doi.org/10.1128/IAI.73.10.6711-6720.2005.
38. **Gallo P, Goncalves R, Mosser DM.** 2010. The influence of IgG density and macrophage Fc (gamma) receptor cross-linking on phagocytosis and IL-10 production. Immunol Lett **133:**70–77. http://dx.doi.org/10.1016/j.imlet.2010.07.004.
39. **Martinez FO, Helming L, Gordon S.** 2009. Alternative activation of macrophages: an immunologic functional perspective. Annu Rev Immunol **27:**451–483. http://dx.doi.org/10.1146/annurev.immunol.021908.132532.
40. **Nimmerjahn F, Ravetch JV.** 2007. Fc-receptors as regulators of immunity. Adv Immunol **96:**179–204. http://dx.doi.org/10.1016/S0065-2776(07)96005-8.
41. **Willcocks LC, Smith KG, Clatworthy MR.** 2009. Low-affinity Fcgamma receptors, autoimmunity and infection. Expert Rev Mol Med **11:**e24. http://dx.doi.org/10.1017/S1462399409001161.
42. **D'Souza WN, Lefrancois L.** 2003. IL-2 is not required for the initiation of CD8 T cell cycling but sustains expansion. J Immunol **171:**5727–5735. http://dx.doi.org/10.4049/jimmunol.171.11.5727.
43. **O'Garra A.** 1998. Cytokines induce the development of functionally heterogeneous T helper cell subsets. Immunity **8:**275–283. http://dx.doi.org/10.1016/S1074-7613(00)80533-6.
44. **Larson RP, Shafiani S, Urdahl KB.** 2013. Foxp3$^+$ regulatory T cells in tuberculosis. Adv Exp Med Biol **783:**165–180. http://dx.doi.org/10.1007/978-1-4614-6111-1_9.
45. **Vignali DA, Collison LW, Workman CJ.** 2008. How regulatory T cells work. Nat Rev Immunol **8:**523–532. http://dx.doi.org/10.1038/nri2343.
46. **Shevach EM, Piccirillo CA, Thornton AM, McHugh RS.** 2003. Control of T cell activation by CD4$^+$ CD25$^+$ suppressor T cells. Novartis Found Symp **252:**24–44.
47. **Gopal R, Lin Y, Obermajer N, Slight S, Nuthalapati N, Ahmed M, Kalinski P, Khader SA.** 2012. IL-23-dependent IL-17 drives Th1-cell responses following *Mycobacterium bovis* BCG vaccination. Eur J Immunol **42:**364–373. http://dx.doi.org/10.1002/eji.201141569.
48. **Ireland SJ, Monson NL, Davis LS.** 2015. Seeking balance: Potentiation and inhibition of multiple sclerosis autoimmune responses by IL-6 and IL-10. Cytokine **73:**236–244. http://dx.doi.org/10.1016/j.cyto.2015.01.009.
49. **McGeachy MJ, Bak-Jensen KS, Chen Y, Tato CM, Blumenschein W, McClanahan T, Cua DJ.** 2007. TGF-beta and IL-6 drive the production of IL-17 and IL-10 by T cells and restrain T(H)-17 cell-mediated pathology. Nat Immunol **8:**1390–1397. http://dx.doi.org/10.1038/ni1539.
50. **Kopf M, Baumann H, Freer G, Freudenberg M, Lamers M, Kishimoto T, Zinkernagel R, Bluethmann H, Kohler G.** 1994. Impaired immune and acute-phase responses in interleukin-6-deficient mice. Nature **368:**339–342. http://dx.doi.org/10.1038/368339a0.
51. **Scheller J, Chalaris A, Schmidt-Arras D, Rose-John S.** 2011. The pro- and anti-inflammatory properties of the cytokine interleukin-6. Biochim Biophys Acta **1813:**878–888. http://dx.doi.org/10.1016/j.bbamcr.2011.01.034.